Seismicity of North-western Namibia during the Period 01 January to 31 May 2012

Bufelo Lushetile[1] and Graham Stuart[2]

1. Geological Survey of Namibia, Geophysics Division, 6 Aviation Road, Windhoek, Namibia
<Bufelo.Lushetile@mme.gov.na>
2. University of Leeds, School of Earth and Environment, Woodhouse, Leeds, UK
<G.W.Stuart@leeds.ac.uk>

Abstract :- The aim of this study was to investigate the seismicity of north-western Namibia, which correlates with a zone of predicted long-term average high strain rates. Consequently, the local seismicity was monitored over a five month-period (01 January – 31 May 2012) to determine how seismically active the area actually is. During this time a total of 281 earthquakes, 149 of which were aftershocks, with local magnitudes from -0.4 to 4.7 M_L were recorded. Analysis centred upon events surrounding the earthquake which occurred on March 24, 2012 (origin time 4:43:52, location -20.127° S / 14.461° E, depth of 0.1 km and magnitude 4.7 M_L) approximately 60 km northwest of Khorixas, in order to identify precursors, if any, as well as the sequence of aftershocks. The present investigation revealed a new seismic zone characterised by smaller magnitude earthquakes, named here the Kamanjab Seismic Zone. The study is part of the WALPASS project which deployed 40 temporary seismic stations on- and offshore north-western Namibia from October 2010 to November 2012. Its goals were to image the lithosphere and deeper upper mantle in the ocean-continent transition beneath the passive continental margin of northern Namibia, and to detect seismic anomalies.

Keywords :- Seismicity; Earthquake; Kamanjab Seismic Zone

Introduction

Seismicity in Namibia is considered to be low to moderate (Fig. 1), the first earthquake having been recorded in 1910. Before the establishment of the Namibian Seismological Network (NSN) in 2002, the country only had two seismic stations, located in Tsumeb and Windhoek, which were operated by the United States Geological Survey (USGS) and the Worldwide Standardised Seismological Network (WWSSN), respectively (Mangongolo and Hutchins, 2008). This sparse seismic network meant that only larger earthquakes were documented, while smaller ones that are easily attenuated, remained undetected. Although, by 2010 the NSN had increased to eight permanent seismic stations, this was still inadequate for a huge country like Namibia, with a low population density. For this reason, the WALPASS (Walvis Ridge Passive Source Seismic Experiment) Project was initiated by GFZ (Deutsches GeoForschungsZentrum), which deployed 12 ocean-based (OBS) and 28 land-based (LBS) temporary broadband seismic stations between October 2010 and November 2012, offshore and onshore north-western Namibia (Fig. 2). The project was aimed, firstly, at imaging the structure of the crust and upper mantle beneath the passive continental margin of northern Namibia and, secondly, at finding seismic anomalies related to the postulated hotspot track from the continent out into the South Atlantic Ocean along the Walvis Ridge (Heit *et al.*, 2012). In addition, the data generated by this project was used to study and analyse the seismic activity of north-western Namibia.

Geological Setting

The study area spans a portion of the Damara mobile belt, which consists of a coastal arm (Kaoko Belt) and a NE-SW striking intracontinental arm (Damara Belt *sensu stricto*; e. g. Porada, 1979). The coastal Kaoko Belt and the intracontinental Damara Belt are genetically individual orogens joined together during the amalgamation of Western Gondwana (Porada, 1989; Fig. 3). The two orogens have distinct structural trends and styles. While the Kaoko Belt with its NNW-trending structural grain resulted from oblique, south-westerly subduction of the Congo Craton beneath the South American Craton, the ENE-trending Damara Belt developed during collision of the south-eastern Kalahari and north-western Congo Craton (Gray *et al*., 2008). Both, the Kaoko and Damara Belt consist of a number of distinct, fault- or thrust-bounded tectonostratigraphic zones characterised by deformation style, metamorphic grade and lithology (Fig. 4), with the junction of the two branches, southwest of Khorixas, displaying complex deformation patterns (Gray *et al*., 2008). The south-west African passive margin originates from the break-up of the Gondwana supercontinent, which in western Gondwana began during the Early Cretaceous (Ewart *et al*., 1998).

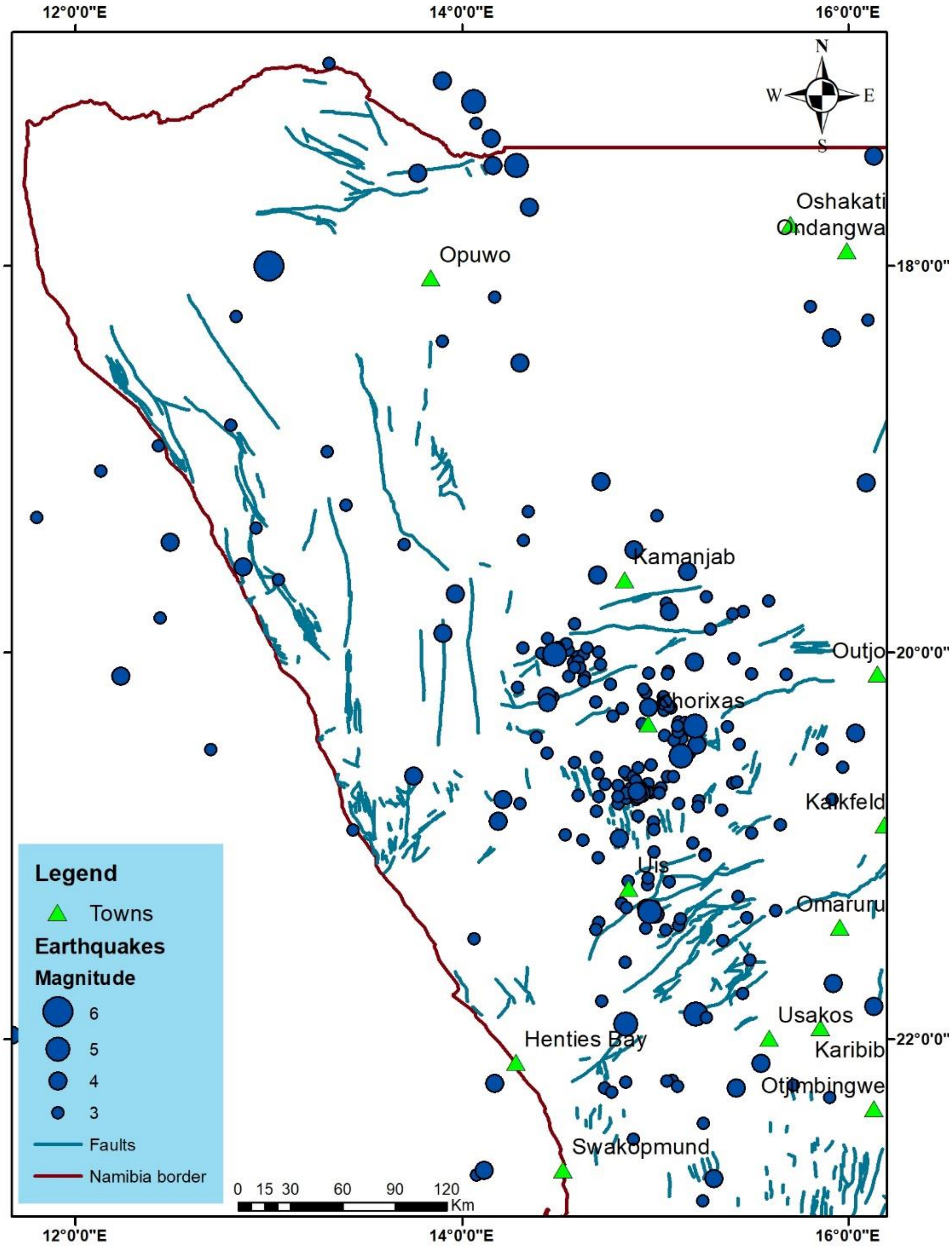

Figure 1. Seismicity of north-western Namibia (International Seismology Centre, ISC)

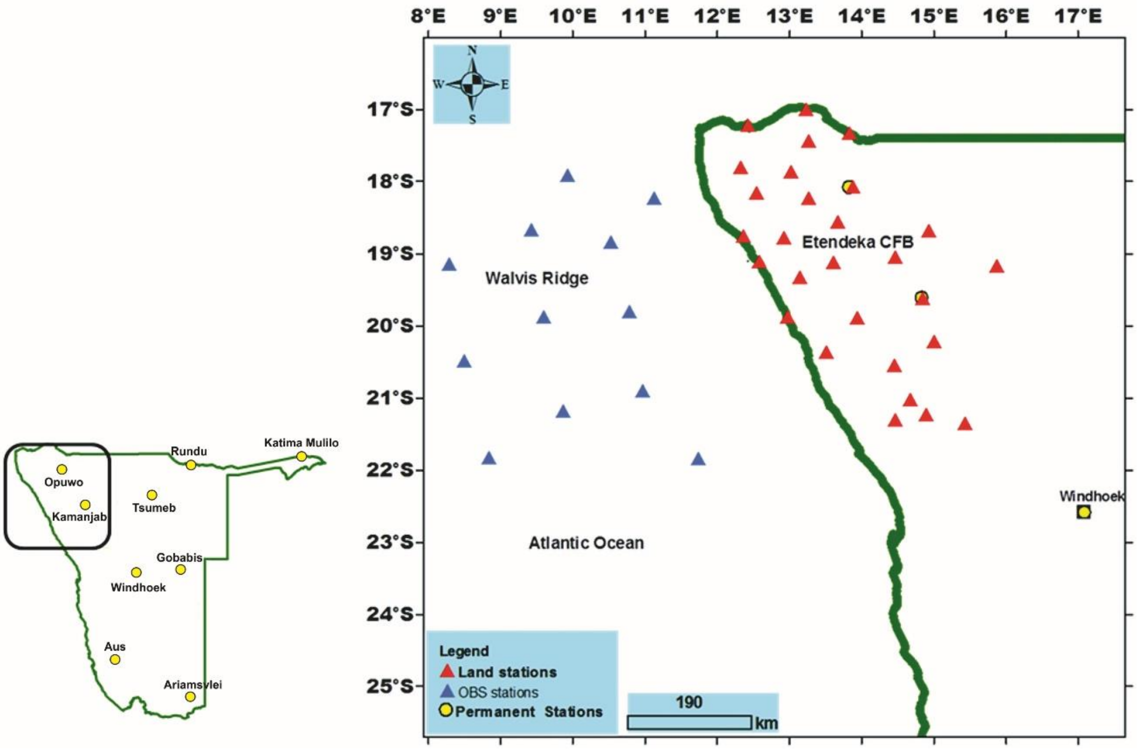

Figure 2. Temporary seismic network deployed by the WALPASS project showing the 12 ocean-based (OBS) and 28 land-based (LBS) stations; left: NSN permanent stations (yellow dots) and extent of the study area

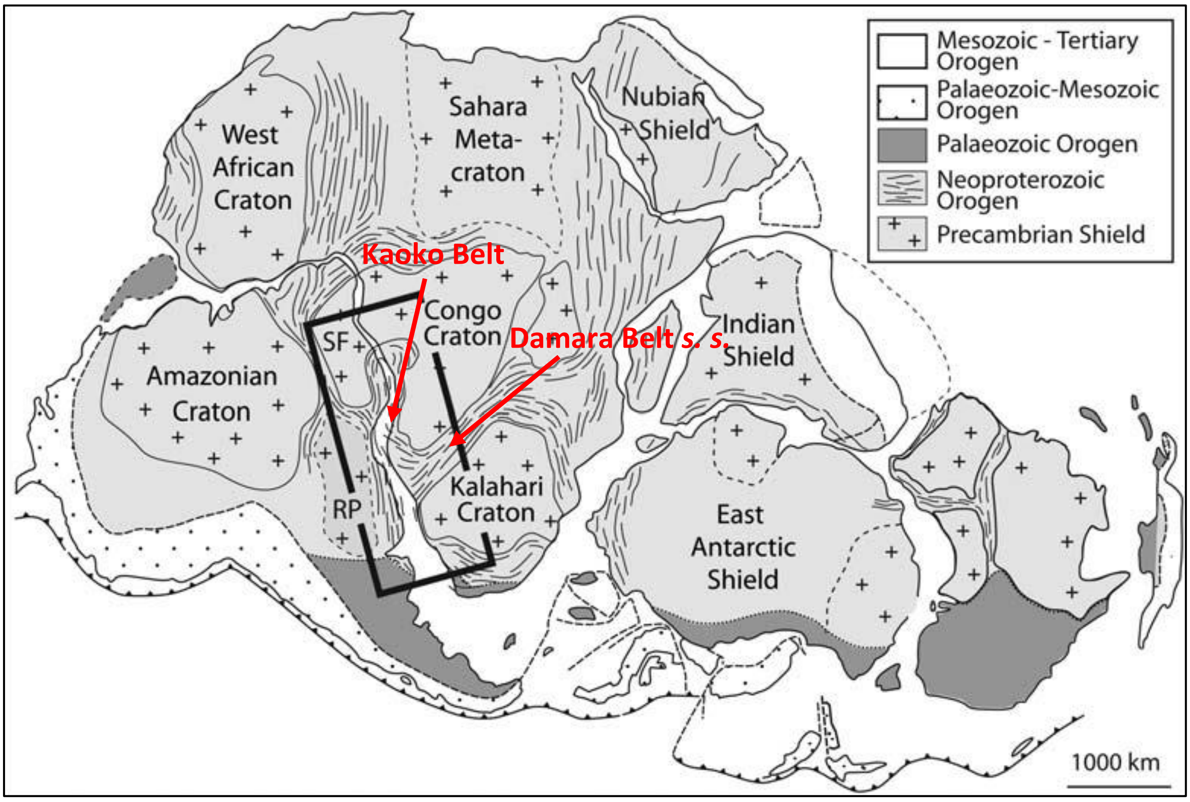

Figure 3. Schematic map of the Gondwana supercontinent showing the positions of cratons and orogenic belts (after Gray *et al*., 2008)

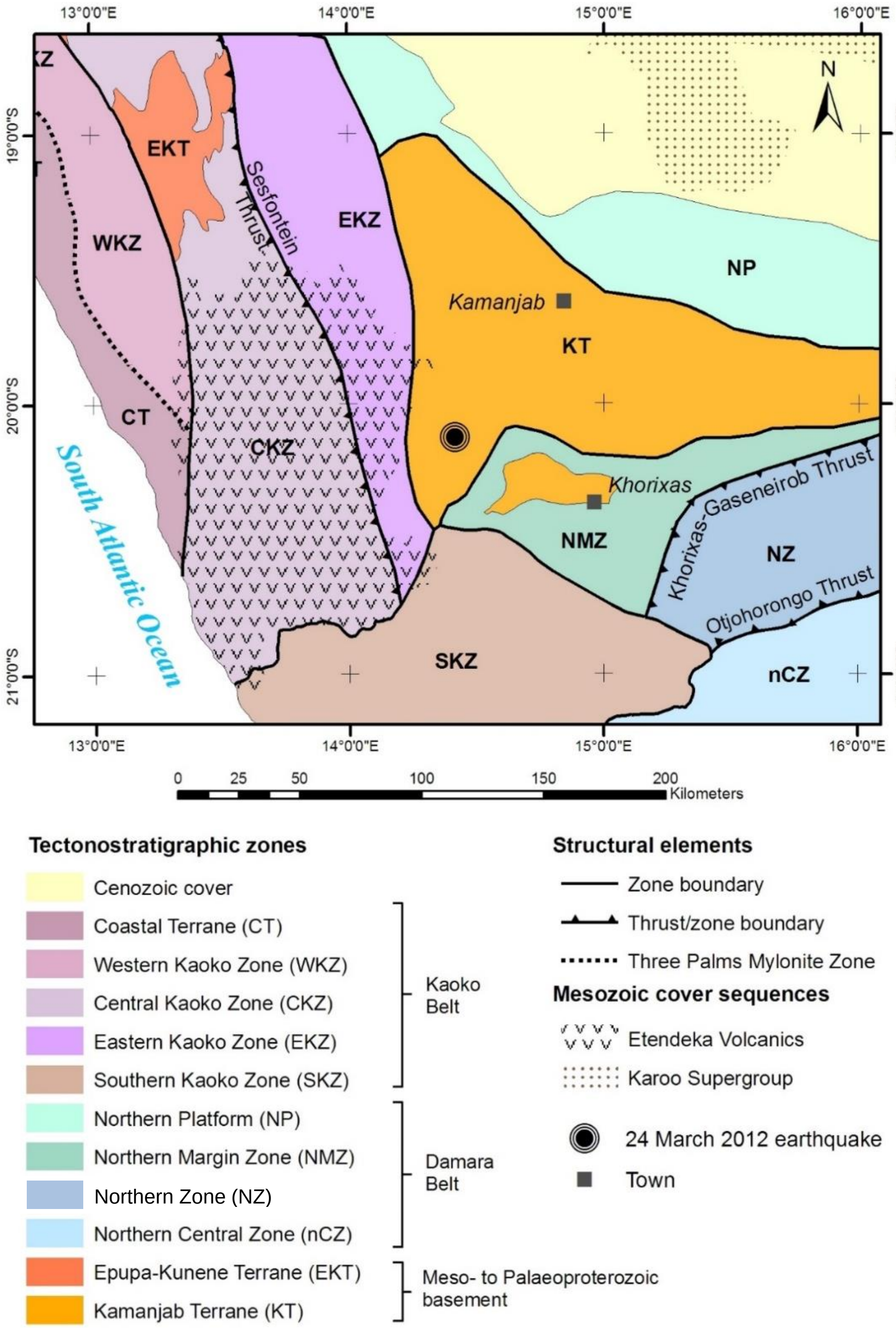

Figure 4. Location of the 24 March 2012 earthquake in relation to the tectonostratigraphic framework of north-western Namibia: the epicentre is situated within the Palaeoproterozoic Kamanjab basement inlier consisting of metamorphosed volcanic, sedimentary and intrusive rocks, near the juncture of the Neoproterozoic Damara and Kaoko orogenic belts. During the Damara Orogeny the area underwent complex multiphase deformation, with some of the lineaments and structures being rejuvenated during the Mesozoic and break-up of the Gondwana Supercontinent (Miller, 2008).

Regional seismicity

Seismicity studies in Namibia relating epicentre locations to known geological faults and fault systems were conducted by Mangongolo and Hutchins (2008), based on historical seismic data from the Council for Geoscience (South Africa), the United States Geological Survey, the International Seismological Centre (UK), the Goetz Observatory (Zimbabwe) and the newly established Seismological Network of Namibia. They concluded that most seismic events occurred along the escarpment separating the central highlands from the coastal plains and in topographically high-lying zones of the Damara and Namaqua orogenic belts, in association with major fault systems. These topographically high regions are part of the Wegener Stress Anomaly (WSA), which extends from south-western Angola to South Africa (Bird *et al*., 2006; Fig. 5).

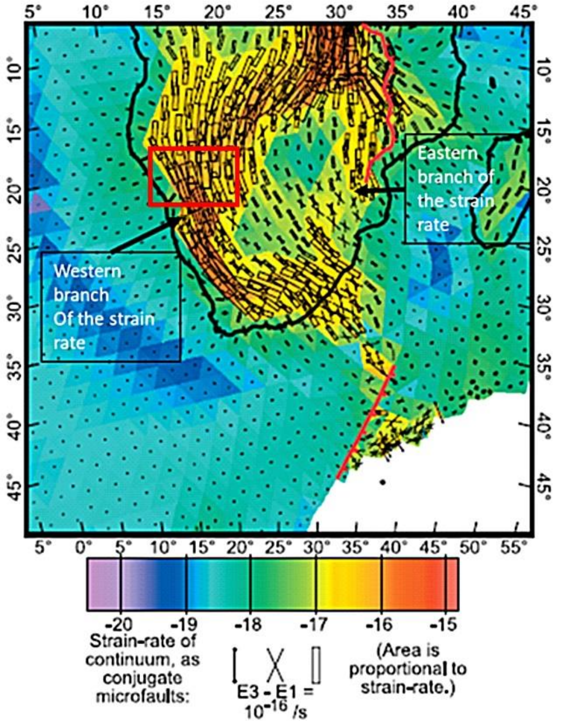

Figure 5. Predicted long-term average strain rates in the study area (red rectangle; after Bird *et al.* (2006); symbols show orientation of the strain rate tensor

Bird *et al.* (2006) carried out modelling experiments to determine the causes of stress in southern Africa and neotectonics of the lithosphere, using the Shell software (Kong and Bird, 1995). Out of eight models tested, the AF-SO-013 model (Fig. 7) was the most preferred, as there was a high correlation between the strain rate field and instrumental seismicity. This model predicts that the Wegener Stress Anomaly is represented by a SW-NE compressive horizontal principal stress direction (σ_{2H}), exceeding the NW-SE compression (σ_{1H}); it further predicts a dominant normal faulting and minor thrusting stress regime for the study area (Fig. 6).

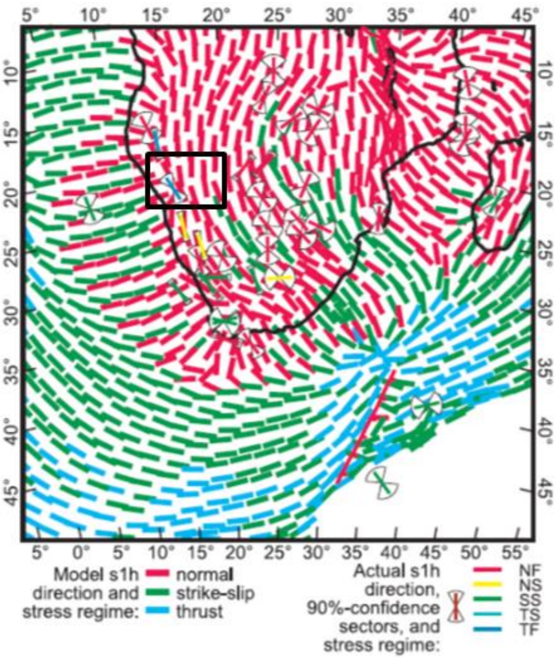

Figure 6. Mostly compressive horizontal principal stress direction from the preferred model AF-SO-013 (Fig. 7), shown as thrust regime in southern Africa and Madagascar (Bird *et al*., 2006); black polygon indicates the study area

The WSA is thought to be the result of ridge-push from the South-west Indian Ridge caused by unbroken lithosphere resistance to rotation between the Somalia and Africa Plates (Bird *et al*., 2006; Fig 7). The strain rate and stress direction of the western branch connects to a western arc extending through Angola, Namibia and South Africa, while the eastern branch joins with a less active south-eastern fan passing through offshore northern Mozambique (Fig. 5).

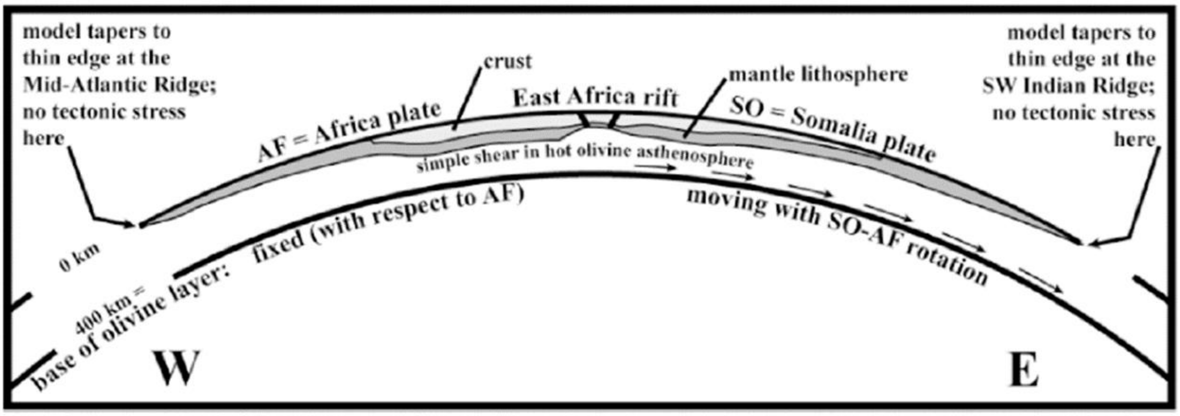

Figure 7. Schematic cross-section through the preferred model AF-SO-013 along an east-west great circle, showing a divergent flow assumed to drive relative rotation of the Somalia Plate with respect to the Africa Plate (Bird *et al*., 2006; cross-section not to scale)

Location methods and velocity models

In the present study the HYPOCENTER software (Lienert and Havskov, 1995; Lienert *et al*., 1986), which combines most features of the HYPO71 and HYPOINVERSE software, was employed. This software calculates the location (x,y,z) and origin time (t_0) for a single event by tracing the rays through a given 1-D velocity model (both direct and refracted waves), and adjusting earthquake parameters using a conventional least-squares approach (Gubbins, 2004).

To improve the accuracy of hypocentre locations, known blasts at the Navachab, Rössing and Langer Heinrich Mines were used to test for the optimal velocity model. Two velocity models, i. e. a crustal model, which is the 1-D global velocity model in the SEISAN software (Havskov and Ottemoller, 1999), and the 1-D IASP91 velocity model were tested. Mine events with at least five clearly observable P and S arrivals were selected, with an average of 10 phase readings for each event. Events with root mean square (rms) residuals larger than 1 s and standard location errors (horizontal error – ERH; vertical error - ERZ) larger than 3 km were rejected. The tests showed that the IASP91 velocity model located the mine blasts more precisely than the crustal model.

Results

The seismicity pattern of north-western Namibia determined by the current study is similar to that observed by Mangongolo and Hutchins (2008). However, in addition to the Windhoek Graben - Okahandja Lineament and the North-western Seismic Zone, a new zone was identified west of Kamanjab, referred to here as the Kamanjab Seismic Zone (Fig. 8). Of the 281 earthquakes recorded during the period January to May 2012 the majority occurred within this zone, including the main 24 March earthquake. Events decrease away from the main quake, but isolated occurrences are observed to the south and north (Fig. 9).

The main event during the study period was relocated with better accuracy on account of the improved seismic station distribution: occurring at 4:43:52 on 2012/03/24, it was located at 20.127° S, 14.461° E and depth 0.1 km. The average uncertainties in the determination of hypocentre location were 5.48 km in the horizontal and 5.42 km in the vertical direction due to the limitations of manually picking P and S waves of small magnitude events. The area of occurrence is sparsely populated, with the nearest town Khorixas situated some 60 km to the southeast. Other populated places at some distance from the epicentre are Palmwag, ~40 km to the northwest, Kamanjab, ~70 km to the northeast and Fransfontein, ~60 km due east. The farthest location from which repercussions were reported is Henties Bay, some 220 km to the south. There was no report of injury or death associated with the event, only relatively minor damage to property such as broken windows and falling dishes.

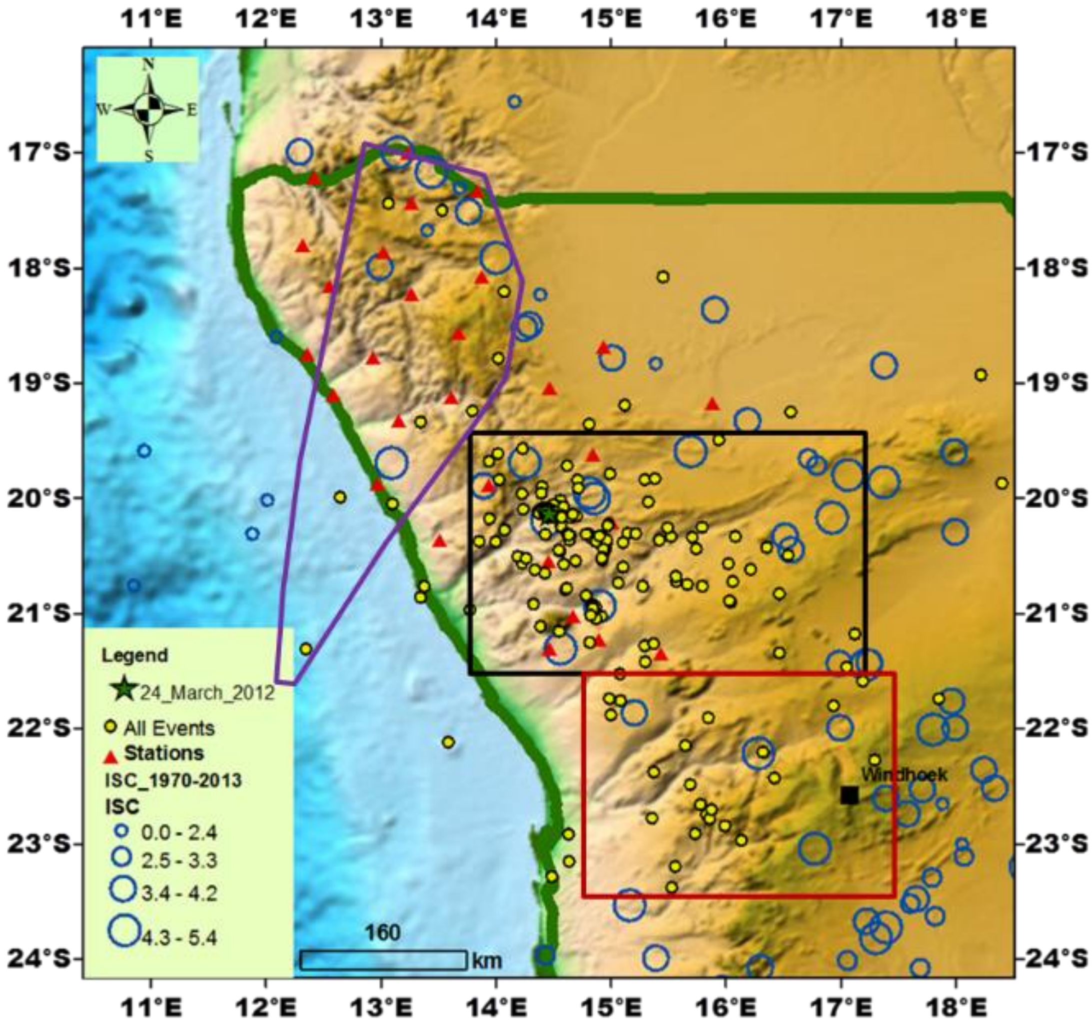

Figure 8. Seismicity in relation to known active seismic zones in Namibia: north-western seismic zone (purple polygon); Windhoek Graben and Okahandja Lineament (red rectangle); Kamanjab Seismic Zone (black rectangle). Red triangles denote temporary seismic stations; ISC events are represented by open circles. The fact that few events have been recorded in the north-western part of the network may be attributed to a lower earthquake frequency and/or sparse seismic recording stations.

Kamanjab Seismic Zone

A rectangle (measuring 392 km²; Fig. 9) within the newly identified Kamanjab Seismic Zone was chosen in order to determine local magnitudes, frequency distribution (Fig. 10) and focal plane solutions (Fig. 11). A total of 111 events occurred in this zone during the study period, with the earliest earthquake recorded on 27th February and the last on 19th May 2012. Apart from the main 4.7M_L event, most earthquakes were very minor, with the smallest recorded at -0.4 M_L and the second largest at 3.9 M_L. The local magnitude scale is calculated as $\log A - 2.48 + \log \Delta$, where A is the amplitude of the signal and Δ the epicentral distance (Lay and Wallace, 1995). In the case of very small earthquakes, with small amplitudes and short epicentral distances, the local magnitude will be negative, because of logarithm of smaller numbers and a regional scale factor that is already negative. Small earthquakes produce seismic waves that can only be detected by modern seismographs. Figure 9 shows a NW-SE alignment of the earthquakes recorded during the study period, indicating the location of causative faults which, however, do not correspond with any mapped structures. It is concluded, therefore, that the causative faults either do not find expression at the surface, or that available geological mapping in the area is not sufficiently detailed.

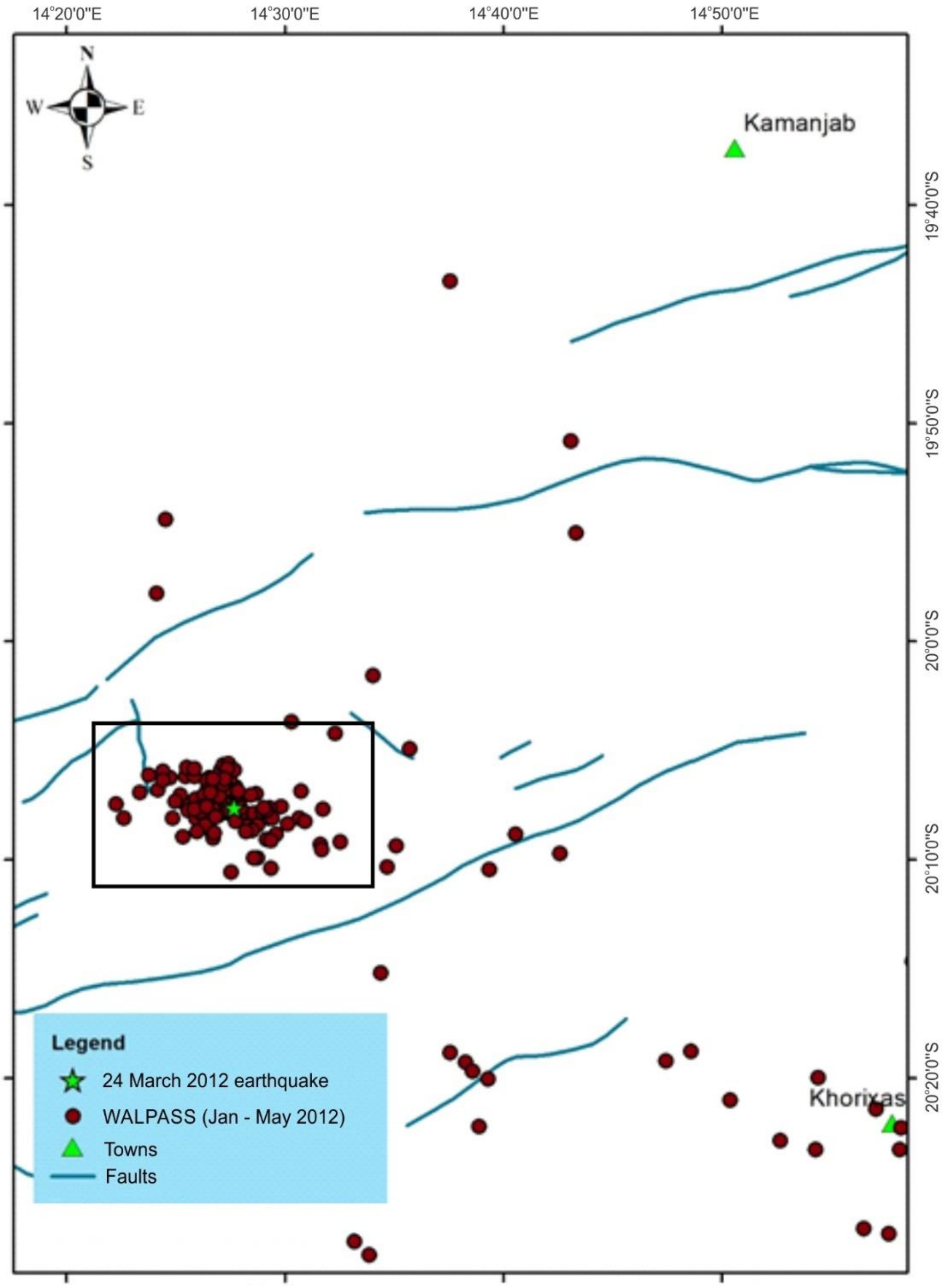

Figure 9. Close-up of events within the Kamanjab Seismic Zone showing a NW-SE oriented cluster (black rectangle) and mapped faults around the seismic zone; green star = location of the main 24 March earthquake

Frequency-Magnitude distribution

The Gutenberg - Richter relation provides a statistical distribution of earthquake magnitudes and is described by a power law (Gutenberg and Richter, 1944):

$$\log_{10} N = a - bM$$

where N is the number of earthquakes in a group having magnitudes larger than M, **a** is a constant and **b** is the slope of the log-linear relation.

In our study, the b-value, which represents the percentage of existing stress to the final breaking stress within the fault (Scholz, 1968), was 0.75 (Fig. 10), which is low compared to values typical for seismically active regions (≥ 1). This may be indicative of a stable crustal region with less fractured crust, or else of an incomplete earthquake catalogue leading to biased results. For the WALPASS project the cut-off was M_L 1.8, below which events could not be reliably detected.

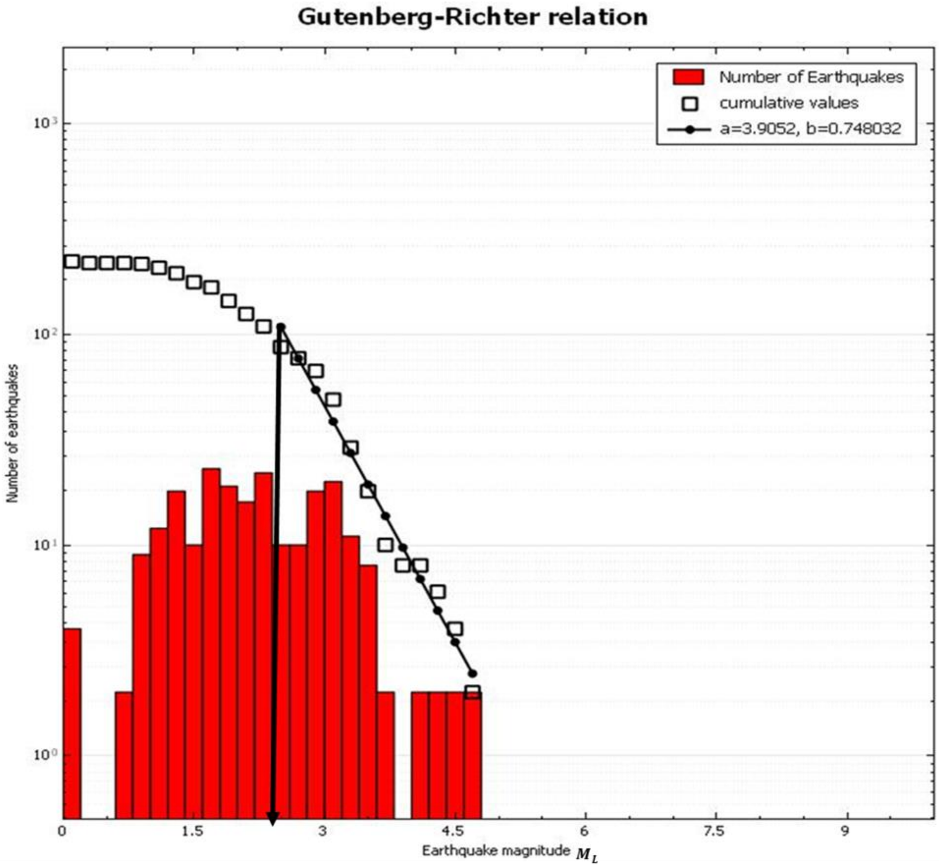

Figure 10. Frequency - magnitude correlation of events in the Kamanjab Seismic Zone showing 1.8 M_L cut-off

Fault plane solutions

Focal mechanisms give the fault plane orientation and slip direction of seismic events, and provide information about the investigated fault and the stress field in which it occurs (Hardebeck and Shearer, 2003). The focal mechanism solution of the main 24 March 2012 earthquake obtained from P arrivals indicates normal faulting (Fig. 11a). Eighteen stations were used with good signal to noise ratios. The focal mechanism solution yielded strike = 0°, dip = 34° and rake = 90°, pointing to a shallow normal fault dipping to the east and striking north-south. Generally, major faults and lineaments in the study area are oriented in NW-SE direction (Gray *et al*., 2008); however, near the study area faults tend to stike NE-SW (Fig. 9).

The second event, which occurred on 24 March 2012 at 05:02 has a focal solution with strike = 59°, dip = 44° and rake = -66°, suggesting a transtensional stress regime (Fig. 11b), which is not in agreement with Grey *et al*. (2008), who stated that most of the Damara Belt is dominated by craton-bound, imbricate thrust shear zone systems with complex fold interference trending NNW. Chetty (2017) asserts that transpression and transtension are strike-slip deformations that deviate from simple shear and are widespread in orogenic belts. These stress regimes occur at local and regional scale but typically at plate boundaries. The third event happened on 24 March at 06:05 and has a focal solution with strike = 138°, dip = 51° and rake = 53°, which indicates a transpressional stress regime (Fig. 11c).

All focal mechanism solutions show different stress regimes, with the main event indicative of normal faulting. In contrast to expectations, it was found that the aftershocks did not have the same focal mechanism solutions, i. e. the same radiation patterns as the mainshock (Fig. 12). The reason could be that the aftershocks did not occur along the same fault as the mainshock (Barth *et al*., 2008), as might be the case in a structurally complex area such as the junction of two orogenic belts.

The complex deformation and fracture patterns at the juncture of the Kaoko and Damara Orogenic Belts would be expected to result in a heterogeneous velocity structure, affecting focal solutions of shallow earthquakes and presenting challenges to their interpretation.

More focal mechanism solutions, through calculation of higher degree moment tensors and a grid search of stress models, are needed to constrain and select an appropriate focal mechanism (Barth *et al*., 2008; Stein and Wysession, 2009).

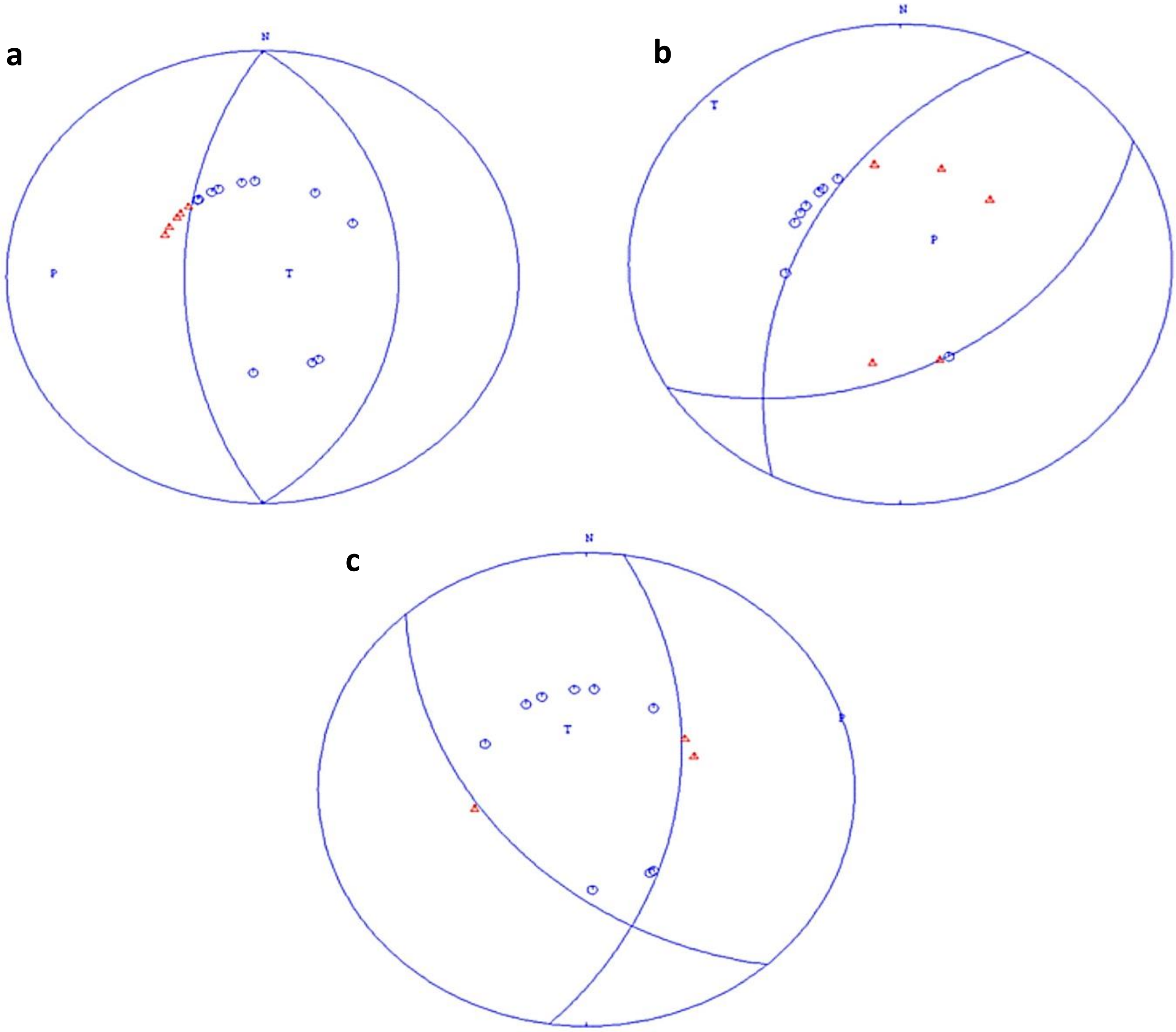

Figure 11. Focal mechanisms of the main 24 March 2012 earthquake: a) at 04:43 showing normal faulting, and an eastward dip; b) at 05:02 showing a transtensional stress regime; c) at 06:05 showing a transpressional stress regime. The red triangles show first motion as compressions (P); blue circles show dilations (T).

Discussion

Foreshocks and aftershocks

116 events occurred before and 165 after the mainshock on 24 March 2012, including those in the Kamanjab Seismic Zone. However, the qualification of an earthquake or tremor as an aftershock requires the specification of time and space windows. Accordingly, a rectangle was drawn around the study area based on the proximity of events to the mainshock and possible seismic event patterns (Fig. 9). Events occurring within this rectangle were analysed to determine foreshocks and aftershocks of the mainshock. 53 foreshocks and 119 aftershocks occurred in the demarcated area, with most of them aligning in NW-SE direction. Foreshocks in appear to have started rupturing early in January 2012 with an increase in frequency, suggesting that the mainshock and the region of foreshock are within the same sequence of cascading ruptures triggered by a common mechanism (Schuh and Böhm, 2011). In addition, several foreshocks were observed around the

mainshock, which, together with the above-mentioned foreshocks, may be associated with stress build-up in and around the fault prior to the main rupture (Fig. 13).

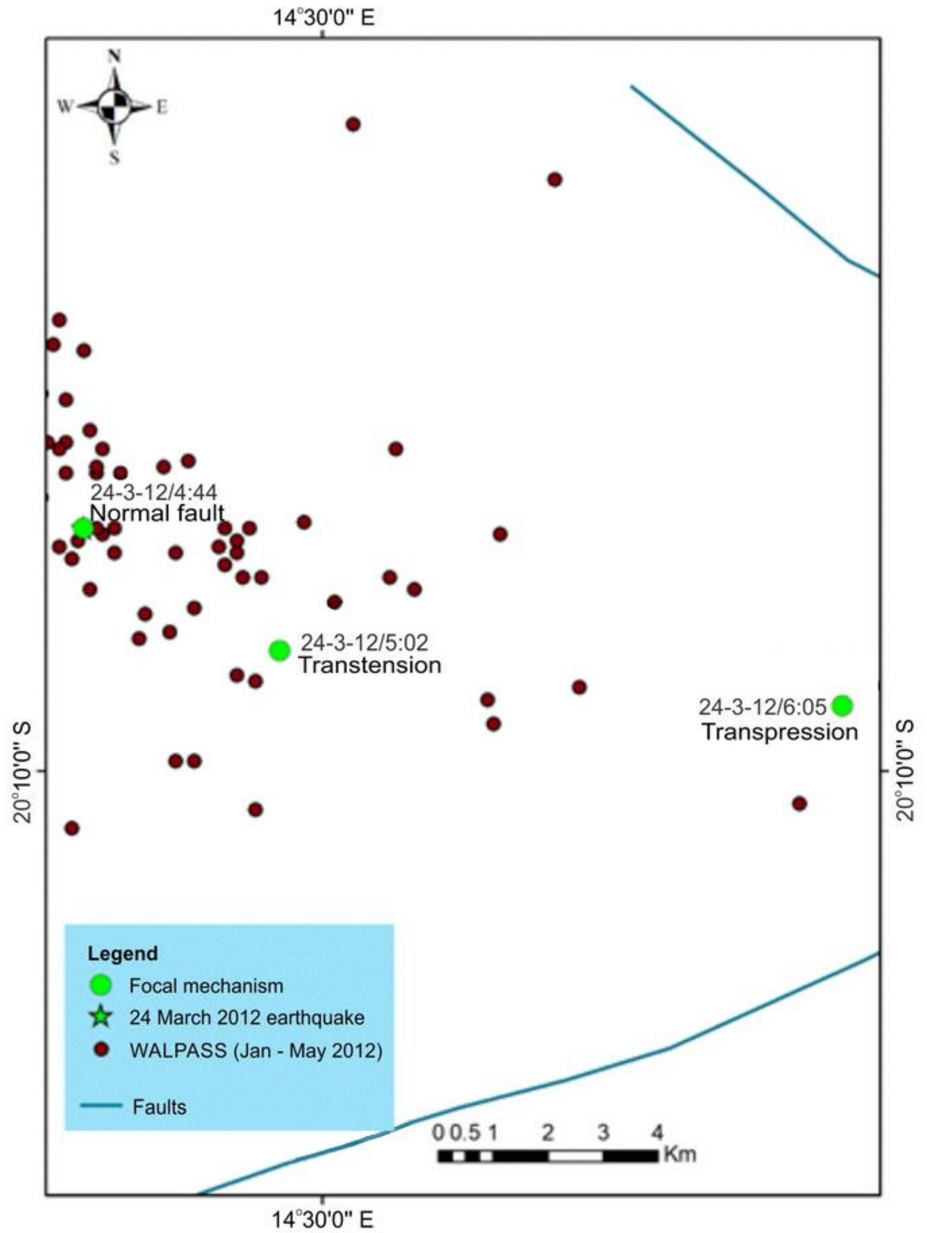

Figure 12. Location of focal mechanism solutions of the 24 March 2012 earthquake (green circles), indicating date, time and stress regime of the event.

Aftershocks occur on planes of weakness in regions of increased post-seismic stress, at the edge of unbroken barriers and in regions of rapid transition from high to low slip around the mainshock (Das and Henry, 2003). In this study, most aftershocks occurred within 10 km of the mainshock rupture, indicating regions of increased stress as a result of the main earthquake. These aftershocks are aligned along the cluster identified in figure 9. Aftershocks larger than 3.5 M_L were plotted, and four of them occurred on the same day as the mainshock. These events are located at the periphery of the cluster (Fig. 14), indicating areas of increased stress. Most of the larger events show a NW-SE linear trend to the north of the mainshock. It is thought that these aftershocks are the result of incomplete rupture, and of the fault(s) readjusting by relieving elastic strain. Most aftershocks are located around the mainshock (Fig. 14).

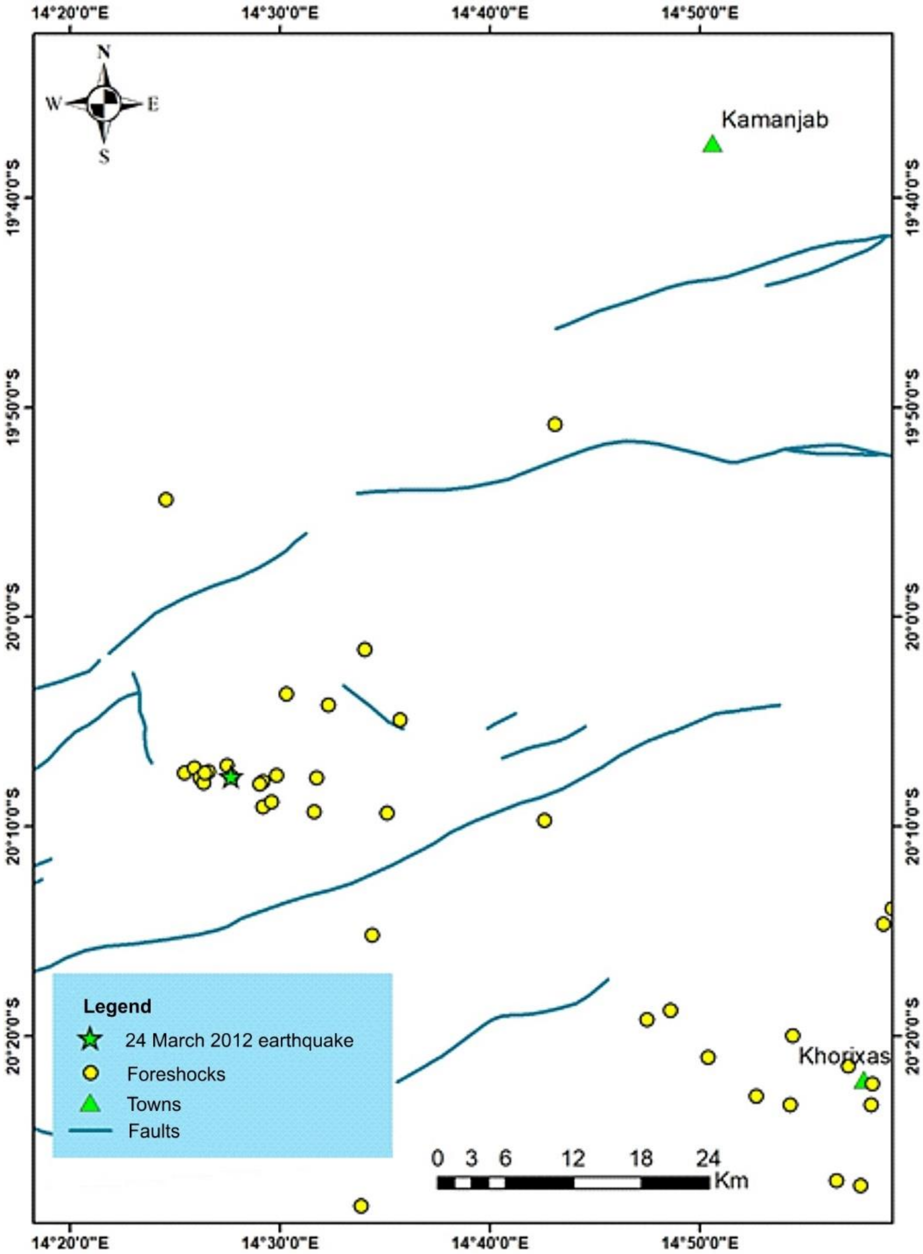

Figure 13. Foreshocks in relation to the main event (green star) showing NW-SE orientation

Regional strain correlation

Judging from the seismicity recorded during the five-month period under consideration, the seismic hazard in north-western Namibia is much higher than predicted by Bird *et al*. (2006), although these observations may not be representative of long-term activity. Study of the entire two year-dataset of the WALPASS project's duration might give a better indication of the latter. However, there is a very strong correlation between the strain rate model predicted and events registered, confirming that seismicity in this region is higher than recorded by current instrumentation.

The AF-SO-013 model prediction in terms of stress and strain in the study area is consistent with our results. Therefore, the above model could be considered as a reliable first order indicator of stress patterns in southern Africa, especially in areas where instrument records are lacking, as, for example, in southern Angola.

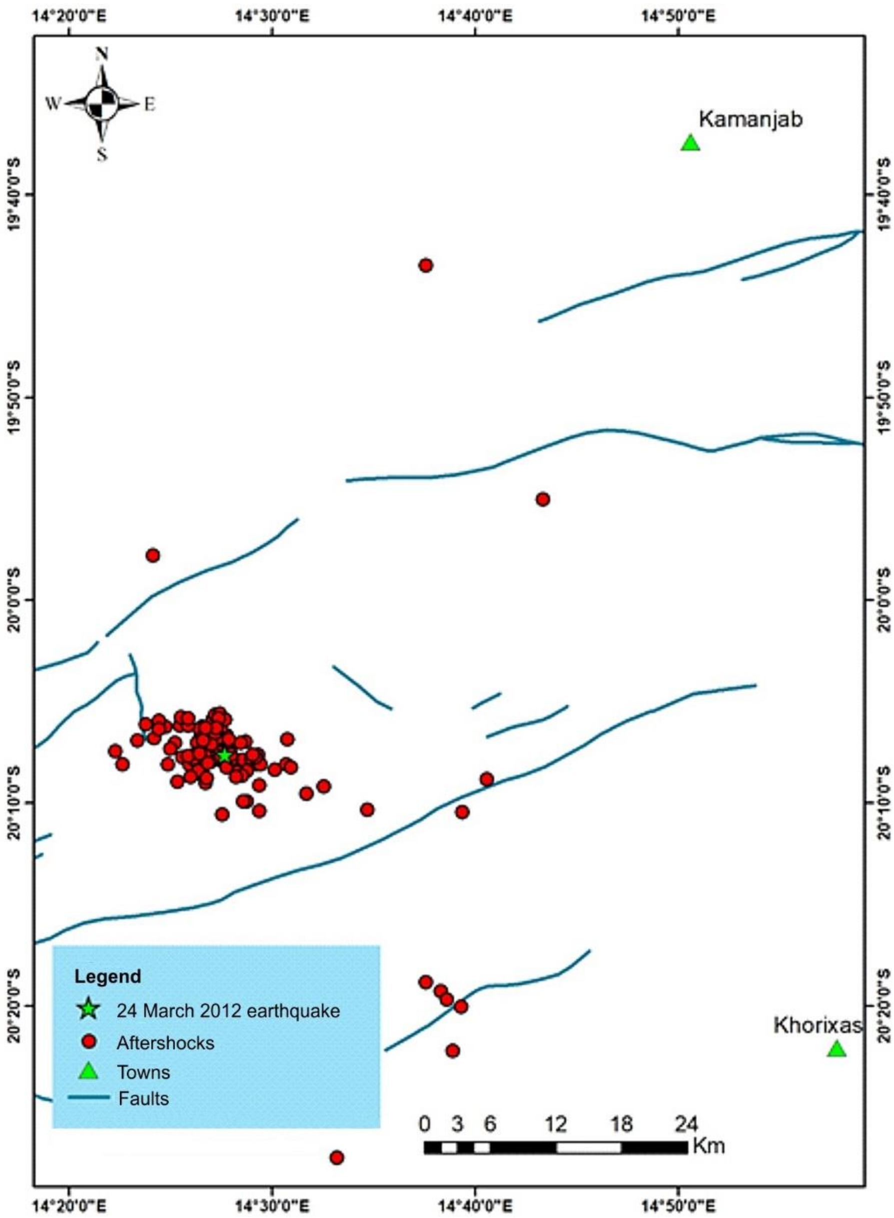

Figure 14. Aftershocks in relation to the main event (green star) extending in a NW-SE orientation

Conclusion

Seismicity observed during the study period indicates a higher earthquake frequency than previously recorded by the NSN stations, with local magnitudes ranging from -0.4 to 4.7 in the newly recognised Kamanjab Seismic Zone. The historic low seismicity records can therefore be attributed to insufficient permanent stations in the area, as most earthquakes with local magnitudes of ≤ 3 M_L are too small to be detected by the current station layout. Two clusters, oriented NE-SW and NW-SE, within the Kamanjab Seismic Zone, are likely due to complex faulting, and indicative of directions of high recent stress within the Palaeoproterozoic basement of the Kamanjab Inlier. Recorded foreshocks heralded the main event on 24th March 2012, with a rupture pattern of seismic activity extending from south-east of the mainshock towards the Kamanjab Seismic Zone, and alternating periods of quiescence and high activity.

There is a marked correlation between the recorded seismicity in the study area and the predicted strain model that connects the western branch of the East Africa Rift System to Angola, Namibia and South Africa (Fig. 5). However, since only five months of data were used in this analysis, a further study of local events over the entire two-year duration of the WALPASS project would be needed to verify the existence of a higher seismicity and tectonic stress patterns in north-western Namibia than is indicated by the recordings of the current permanent station network.

References

Barth, A., Reinecker, J. and Heidbach, O. 2008. Stress derivation from earthquake focal mechanisms. *World Stress Map Project Guidelines*. https://www.world-stress-map.org

Bird, P., Ben-Avraham, Z. Schubert, G., Andreoli, M. and Viola, G. 2006. Patterns of stress and strain rate in southern Africa. *Journal of Geophysical Research: Solid Earth*, **111(B08),** https://doi.org/10.1029/2005JB003882

Chetty, T. R. K. 2017. *Proterozoic Orogens of India: A Critical Window to Gondwana*. Elsevier.

Das, S. and C. Henry, C. 2003. Spatial relation between main earthquake slip and its aftershock distribution. *Reviews of Geophysics*, **41(3)**, https://doi.org/10.1029/2002RG000119

Ewart, A., Milner, S. C., Armstrong, R. A. and Duncan, A. R. 1998. Etendeka volcanism of the Goboboseb Mountains and Messum Igneous Complex, Namibia. Part I: Geochemical evidence of early Cretaceous Tristan Plume melts and the role of crustal contamination in the Paraná–Etendeka CFB. *Journal of Petrology*, **39(2)**, 191-225.

Gray, D. R., Forster, D. A, Meert, J. G., Goscombe, B. D., Armstrong, R., Trouw, R. A. J. and Passchier, C. W., 2008. A Damara orogen perspective on the assembly of southwestern Gondwana, 257-278. *In*: Pankhurst, R. J., Trouw, R. A. J., De Brito Neves, B. B. and De Wit, M. J. (Eds) West Gondwana: Pre-Cenozoic Correlations Across the South Atlantic Region, *Geological Society Special Publications*, **294**, Geological Society of London, UK.

Gubbins, D. 2004. *Time series analysis and inverse theory for geophysicists*. Cambridge University Press, https://doi.org/10.1017/CBO9780511840302

Gutenberg, B. and Richter, C. F. 1944. Frequency of earthquakes in California, *Bulletin of the Seismological Society of America*, **34**, 185-188.

Hardebeck, J. L. and Shearer., P. M. 2003. Using S/P amplitude ratios to constrain the focal mechanisms of small earthquakes. *Bulletin of the Seismological Society of America*, **93(6)**, 2434-2444.

Havskov, J. and Ottemoller, L. 1999. SEISAN earthquake analysis software. *Seismological Research Letters*, **70(5)**, 532-534.

Heit, B., Yuan, X., Geissler, W., Lushetile, B., Weber, M. and Jokat, W. 2012. The WALPASS - Walvis Ridge Passive-Source Seismic Experiment in Namibia. *Geophysical Research Abstracts*, **14**, (EGU2012-1281-2), General Assembly European Geosciences Union, Vienna, Austria.

Lay, T. and Wallace, T.C. 1995. *Modern Global Seismology*, Academic Press, Cambridge, Ma., 536 pp.

Lienert, B. R., Berg, E. and Frazer, L.N. 1986. HYPOCENTER: An earthquake location method using centered, scaled, and adaptively damped least squares. *Bulletin of the Seismological Society of America*, **76(3)**, 771-783.

Lienert, B. R. and Havskov, J. 1995. A computer programme for locating earthquakes both locally and globally. *Seismological Research Letters*, **66(5)**, 26-36.

Kong, X., and Bird, P. 1995. Shells: A thin-plate program for modelling neotectonics of regional or global lithosphere with faults, *Journal of Geophysical Research.*, **100(B11),** 22129-22131.

Mangongolo, A. and Hutchins, D. G. 2008. Seismicity of Namibia from 1910 to 2006. *In*: Miller, R. McG. (Ed.). *The Geology of Namibia*, Vol. **3**, chapter 27, 7 pp. Geological Society of Namibia, Windhoek.

Porada, H. 1979. The Damara-Ribeira Orogen of the Pan-African-Brasiliano cycle in Namibia (Southwest Africa) and Brazil as interpreted in terms of continental collision. *Tectonophysics*, **57(2)**, 237-265.

Porada, H. 1989. Pan-African rifting and orogenesis in southern to equatorial Africa and eastern Brazil. *Precambrian Research*, **44(2)**, 103-136.

Scholz, C. 1968. The frequency-magnitude relation of microfracturing in rock and its relation to earthquakes. *Bulletin of the Seismological Society of America*, **58(1)**, 399-415.

Schuh, H. and Böhm, S. 2021. Earth rotation, 149-155. *In*: Gupta, H. K. (Ed.), *Encyclopedia of Solid Earth Geophysics*, Springer, Cham.

Stein, S. and Wysession. M. 2009. *An Introduction to Seismology, Earthquakes, and Earth Structure.* John Wiley & Sons, Hoboken, New Jersey, 512 pp.